

## Accepted Manuscript

The discovery of potent and selective kynurenine 3-monooxygenase inhibitors for the treatment of acute pancreatitis

John Liddle, Benjamin Beaufile, Margaret Binnie, Anne Bouillot, Alexis A. Denis, Michael M. Hann, Carl P. Haslam, Duncan S. Holmes, Jon P. Hutchinson, Michael Kranz, Andrew McBride, Olivier Mirguet, Damian J. Mole, Christopher G. Mowat, Sandeep Pal, Paul Rowland, Lionel Trottet, Iain J. Uings, Ann L. Walker, Scott P. Webster

PII: S0960-894X(17)30221-4  
DOI: <http://dx.doi.org/10.1016/j.bmcl.2017.02.078>  
Reference: BMCL 24750

To appear in: *Bioorganic & Medicinal Chemistry Letters*

Received Date: 9 January 2017  
Revised Date: 27 February 2017  
Accepted Date: 28 February 2017

Please cite this article as: Liddle, J., Beaufile, B., Binnie, M., Bouillot, A., Denis, A.A., Hann, M.M., Haslam, C.P., Holmes, D.S., Hutchinson, J.P., Kranz, M., McBride, A., Mirguet, O., Mole, D.J., Mowat, C.G., Pal, S., Rowland, P., Trottet, L., Uings, I.J., Walker, A.L., Webster, S.P., The discovery of potent and selective kynurenine 3-monooxygenase inhibitors for the treatment of acute pancreatitis, *Bioorganic & Medicinal Chemistry Letters* (2017), doi: <http://dx.doi.org/10.1016/j.bmcl.2017.02.078>

This is a PDF file of an unedited manuscript that has been accepted for publication. As a service to our customers we are providing this early version of the manuscript. The manuscript will undergo copyediting, typesetting, and review of the resulting proof before it is published in its final form. Please note that during the production process errors may be discovered which could affect the content, and all legal disclaimers that apply to the journal pertain.



## The discovery of potent and selective kynurenine 3-monooxygenase inhibitors for the treatment of acute pancreatitis

John Liddle<sup>\*a</sup>, Benjamin Beaufile<sup>b</sup>, Margaret Binnie<sup>c</sup>, Anne Bouillot<sup>b</sup>, Alexis A. Denis<sup>b</sup>, Michael M. Hann<sup>a</sup>, Carl P. Haslam<sup>a</sup>, Duncan S. Holmes<sup>a</sup>, Jon P. Hutchinson<sup>a</sup>, Michael Kranz<sup>a</sup>, Andrew McBride<sup>c</sup>, Olivier Mirguez<sup>b</sup>, Damian J. Mole<sup>d</sup>, Christopher G. Mowat<sup>e</sup>, Sandeep Pal<sup>a</sup>, Paul Rowland<sup>a</sup>, Lionel Trotter<sup>b</sup>, Iain J. Uings<sup>a</sup>, Ann L. Walker<sup>a</sup>, Scott P. Webster<sup>c</sup>

*a) GlaxoSmithKline, Gunnels Wood Road, Stevenage, Hertfordshire SG1 2NY, UK. b) GlaxoSmithKline, Les Ulis, Paris, France. c) Centre for Cardiovascular Science, University of Edinburgh, UK. d) MRC Centre for Inflammation Research, University of Edinburgh, U.K. e) EastChem School of Chemistry, University of Edinburgh, UK.*

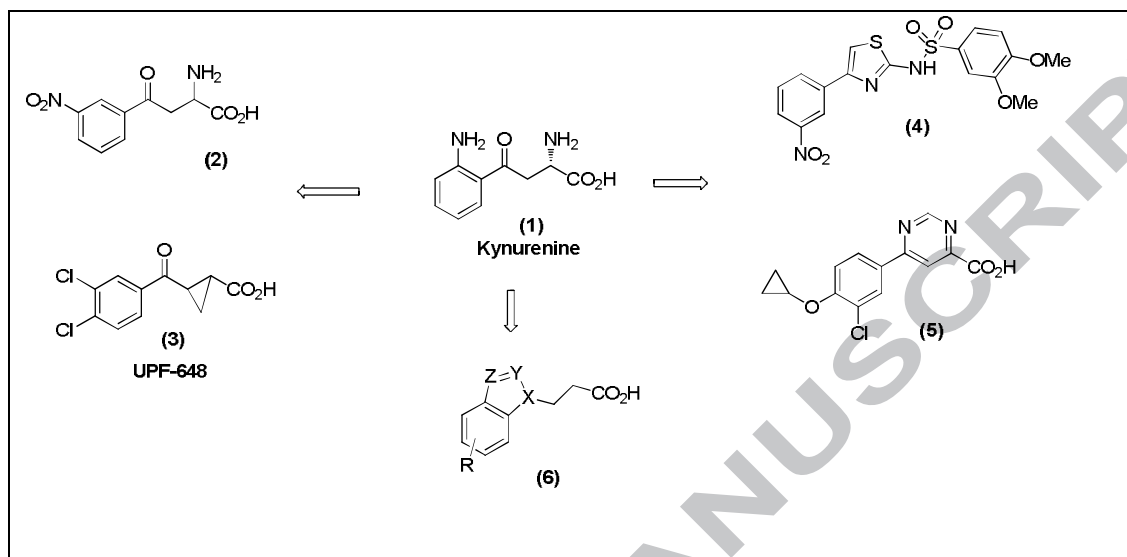
Acute pancreatitis (AP) is an acute inflammation of the pancreas usually triggered by gallstones or excessive alcohol consumption. Approximately 20% of patients will develop a systemic inflammatory response progressing to multiple organ dysfunction syndrome. The mortality rate in this group of patients exceeds 20% with most deaths occurring within the first 7 days of hospital admission.<sup>1</sup> AP remains a significant unmet medical need with the current standard of care being entirely supportive.

A recent prospective study of patients diagnosed with AP showed a strong association between disease severity and the plasma concentrations of the cytotoxic tryptophan metabolite 3-hydroxykynurenine (3HK), which is formed exclusively by kynurenine 3-monooxygenase (KMO).<sup>2</sup> KMO-deficient mice cannot generate 3HK and, compared to wild-type animals, appear resistant to kidney and lung damage when subjected to a model of pancreatic injury driven secondary organ dysfunction.<sup>3</sup> This combination of clinical observation and preclinical rodent model data suggests that the activation of this pathway and the formation of the cytotoxic metabolite 3HK make a significant contribution to the observed pathology. We therefore sought to design potent and selective KMO inhibitors for the treatment of AP with properties amenable to intravenous administration, a requirement for critically ill patients. AP progresses relatively quickly and hence early treatment following clinical diagnosis is important. Our objective therefore was to develop inhibitors with excellent aqueous solubility that could achieve high levels of KMO inhibition rapidly from a single bolus dose. Sustained KMO inhibition would be maintained from a continuous infusion.

KMO is a  $\beta$ -nicotinamide adenine dinucleotide 2'-phosphate (NADPH)-dependent flavin hydroxylase that employs the redox co-factor flavin adenine dinucleotide (FAD) to catalyse the hydroxylation of kynurenine (Kyn) to form 3-HK using molecular oxygen.<sup>4,5</sup> This reaction occurs on the pathway of tryptophan catabolism and leads ultimately to the *de novo* synthesis of the nicotinamide moiety of NAD/NADP. The structure of human KMO has yet to be solved, but a recent paper disclosing the crystal structure of *Saccharomyces cerevisiae* KMO suggests that: i) the phenyl ring of Kyn 1 (Figure 1) occupies a hydrophobic pocket, ii) the carbonyl forms a H-bond to a conserved Gln325 and, iii) the carboxylate forms a salt bridge to Arg83 and H-bond to Tyr97.<sup>6</sup> The aniline is thought to H-bond to

an oxygen atom within the FAD co-factor and the primary amine appears to be devoid of any direct interactions.

**Figure 1:** Substrate derived KMO inhibitors

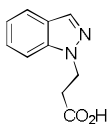
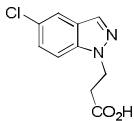
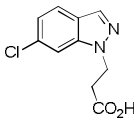
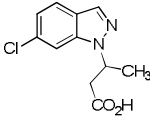
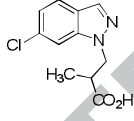
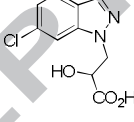
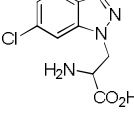
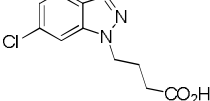
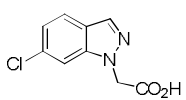


We sought to investigate a substrate-based approach, since Kyn **1** has attractive properties for optimisation including a low molecular weight and low lipophilicity. Indeed, several groups have generated potent KMO inhibitors via a substrate-based approach for the potential treatment of Huntington's disease, but all appeared to lack the physicochemical properties required for the clinical development of an intravenous drug.<sup>7-8</sup> Reports describing the SAR of the kynurenine phenyl ring concluded that 3-chloro, 3,4-dichloro and 3-nitro substituents led to relatively potent KMO inhibitors, exemplified by **2** (KMO IC<sub>50</sub> 900nM; pIC<sub>50</sub> 6.0) and UPF-648 **3** (KMO IC<sub>50</sub> 20nM; pIC<sub>50</sub> 7.7).<sup>9-12</sup> Subsequent generations of KMO inhibitors from Roche **4** and CHDI / Evotec **5** exploited a series of heterocycles to mimic the H-bonding nature of the kynurenine ketone, thought to be important for activity.<sup>13-14</sup>

Our approach focussed on removing the undesirable Kyn aniline and carbonyl moieties by cyclising to form a series of bicyclic propanoic acids, illustrated by **6**. Indeed, the simple indazole **7** (Table 1), which maintains a hydrogen bond acceptor nitrogen in a position similar to the Kyn carbonyl oxygen, had modest activity (pIC<sub>50</sub> 5.2) in the KMO biochemical assay.<sup>15</sup> To confirm the appropriate position for the chloro substituent, which had been reported to increase enzyme inhibition, both the 5-chloro **8** and 6-chloroindazole **9** analogues were prepared. The 6-chloro analogue **9** had a dramatic impact, achieving excellent KMO potency (pIC<sub>50</sub> 7.3), an increase of approximately 100-fold. The 6-chloro substituent was maintained to probe the SAR around the propanoic acid and various bicyclic heterocycles. The propanoic acid chain was sensitive to modification. Introduction of a methyl group, hydroxyl group or amino group at either position on the alkyl chain, exemplified with

analogues **10-13**, was detrimental for potency. Extension of the propanoic chain, compound **14**, was also detrimental although the ethanoic acid **15** showed only a marginal decrease in KMO potency in the indazole series.

**Table 1:** Optimisation of propyl chain

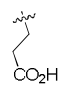
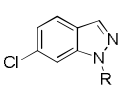
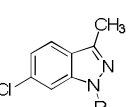
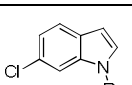
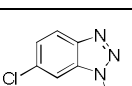
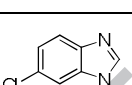
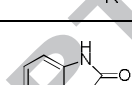
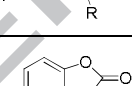
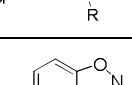
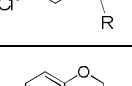
Compound	Structure	KMO enzyme <sup>15</sup> Mean pIC <sub>50</sub> (n)	Ligand efficiency <sup>16</sup>
<b>7</b>		5.2 (7)	0.51
<b>8</b>		6.0 (4)	0.55
<b>9</b>		7.3 (7)	0.67
<b>10</b>		5.3 (3)	0.45
<b>11</b>		5.6 (4)	0.48
<b>12</b>		6.2 (4)	0.53
<b>13</b>		5.6 (7)	0.48
<b>14</b>		5.5 (4)	0.47
<b>15</b>		7.0 (6)	0.69

Compounds **10-13** are racemic mixtures.

Data are given for parent acid, except for **13** which are given for the HCl salt.

KMO enzyme activity was also very sensitive to modification of the core heterocycle, in particular around the 3-position of the indazole (Table 2). Methyl substitution on the 3-position led to a significant loss in potency. The indole **17** maintained comparable potency confirming that the indazole N, postulated to mimic the Kyn carbonyl in H-bonding to Gln 325, was not critical for inhibition.

**Table 2:** Optimisation of heterocyclic core

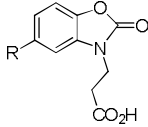
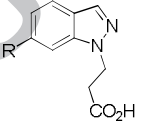
Compound	R= 	KMO enzyme <sup>15</sup> mean pIC <sub>50</sub> (n)	Ligand efficiency <sup>16</sup>
<b>9</b>		7.3 (7)	0.67
<b>16</b>		5.7 (4)	0.49
<b>17</b>		6.9 (6)	0.63
<b>18</b>		6.3 (4)	0.47
<b>19</b>		< 5.0 (3)	NA
<b>20</b>		< 5.2 (10)	0.45
<b>21</b>		7.9 (6)	0.68
<b>22</b>		7.6 (3)	0.69
<b>23</b>		7.1 (6)	0.57

Data are given for parent acid, except for **22** which are given for the 2-amino-(2-hydroxymethyl)-propane-1,3-diol salt

The benzotriazole **18**, benzimidazole **19** and benzimidazolone **20** all lost considerable potency. Interestingly, the introduction of an oxygen atom at the 3-position, as exemplified by the benzoxazolone **21**, benzisoxazole **22** and benzoxazinone **23**, restored good activity.

Before initiating wider exploration of the SAR of the phenyl ring, it was important to confirm that the chloro substituent was optimal. Indeed, chlorine appeared to be the optimal substituent for the 5-position of the benzoxazolone with only a lipophilic bromine atom retaining good enzyme inhibition in the indazole series (Table 3). It is noteworthy that the trifluoromethyl and methyl compounds **26** and **28** lost potency by approximately 100-fold.

**Table 3:** Optimisation of phenyl substituent

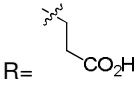
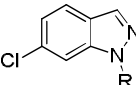
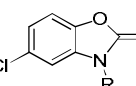
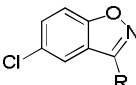
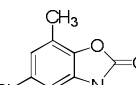
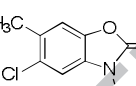
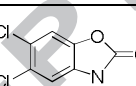
					
Compound	R	KMO enzyme <sup>15</sup> mean pIC <sub>50</sub> (n)	Compound	R	KMO enzyme <sup>15</sup> mean pIC <sub>50</sub> (n)
<b>21</b>	Cl	7.9 (6)	<b>9</b>	Cl	7.3 (7)
<b>24</b>	CN	6.2 (4)	<b>27</b>	Br	7.4 (5)
<b>25</b>	CH <sub>3</sub> O	6.0 (2)	<b>28</b>	CH <sub>3</sub>	5.5 (6)
<b>26</b>	CF <sub>3</sub>	5.3 (4)			

Data are given for parent acid

Although the chloroindazole analogue **9** showed potent KMO inhibition in the biochemical assay, there was no significant inhibition in a cell-based assay using human embryonic kidney (HEK) cells engineered to overexpress human KMO (Table 4).<sup>3</sup> The corresponding benzoxazolone **21** and benzisoxazole **22** analogues, which were marginally more potent in the biochemical assay, showed modest KMO inhibition in the cell assay. Because of high ligand efficiency, encouraging aqueous solubility, photostability and relatively low binding to human serum albumin (HSA), the benzoxazolone core **21** was chosen for further exploration of the SAR with the aim of increasing cellular potency. Further substitution on the phenyl ring was tolerated only at the 6-position. Substitution at the 4 (data not shown) or 7 position was detrimental to enzyme inhibition. The 7-methyl analogue **29** lost approximately 3-fold in potency. The 6-methyl compound **30** (GSK428) maintained good enzyme potency (pIC<sub>50</sub> 7.9) and the increase in lipophilicity (logD 1.3) was accompanied by a significant increase in cellular potency (pIC<sub>50</sub> 6.2), likely due to improved cell

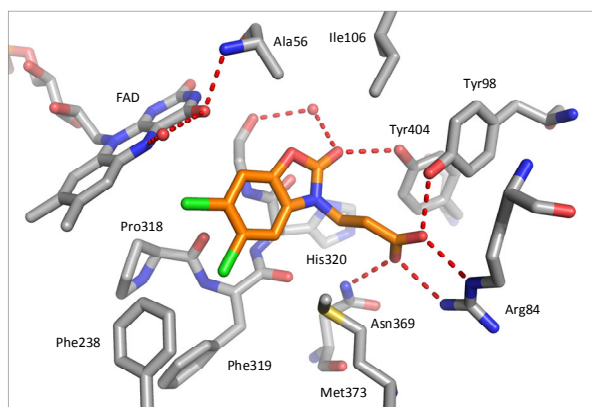
permeability. **30** also maintained a good free fraction in HSA. The introduction of an additional chlorine atom **31** (GSK180) led to excellent enzyme potency although the cell potency was surprisingly disappointing.

**Table 4:** Optimisation of phenyl substituents

Compound	Structure 	KMO Enzyme <sup>15</sup> mean pIC <sub>50</sub> (n)	KMO Cell <sup>3</sup> mean pIC <sub>50</sub> (n)	MW / ChromlogD pH 7.4 <sup>17</sup>	HT Sol (μM) <sup>18</sup>	HSA Binding <sup>19</sup> (%)
<b>9</b>		7.3 (7)	<5.0 (4)	225 / 1.1	>= 207	93.6
<b>21</b>		7.9 (6)	5.4 (3)	242 / 0.8	>= 518	90.8
<b>22</b>		7.6 (3)	5.3 (3)	256 / 1.0	>= 414	97.3
<b>29</b>		7.2 (5)	ND	256 / 1.3	>= 354	94.7
<b>30</b> <b>GSK428</b>		7.9 (13)	6.2 (3)	255 / 1.3	337	95.0
<b>31</b> <b>GSK180</b>		8.2 (6)	5.7 (4)	276 / 1.6	>= 421	96.3

Data are given for the 2-amino-(2-hydroxymethyl)-propane-1,3-diol salt except for **9**, **21** and **31** which are given for the parent acids

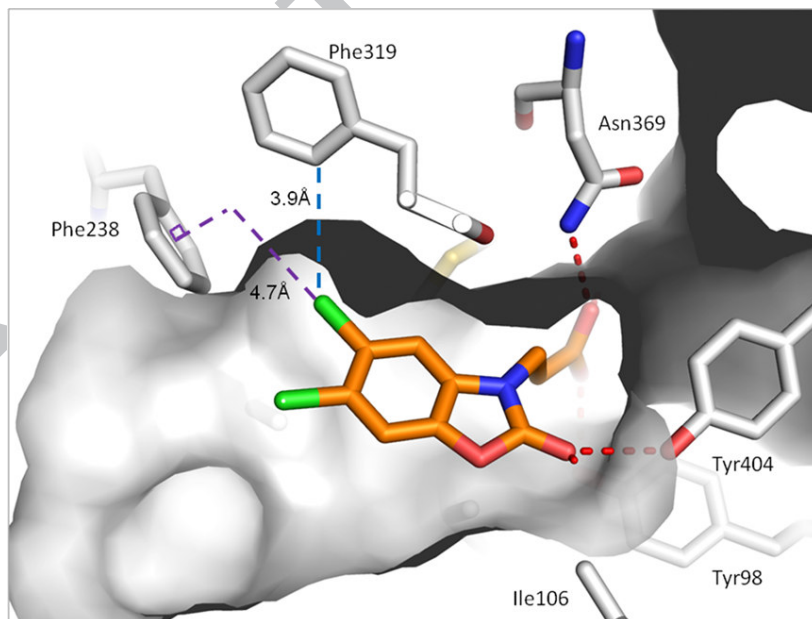
We recently reported a co-crystal structure of **31** bound to *P. fluorescens* KMO.<sup>3</sup> Subsequent work led to a significantly higher resolution (1.8Å) structure being solved (Figure 2).<sup>20</sup> All the residues that surround the catalytic site in the bacterial enzyme are conserved in human KMO, by sequence alignment, with the exception of His320, which is a phenylalanine in the human protein. Despite this high degree of conservation, **31** demonstrated significantly lower potency against *P. fluorescens* KMO compared to human KMO (IC<sub>50</sub> = 500 nM versus 6 nM, respectively). Nonetheless, significant interactions within the catalytic site were revealed: the carboxylate forms a salt bridge with Arg84 and forms a hydrogen bonds with Tyr98 and Asn369; while the oxazolidinone carbonyl forms a hydrogen bond with the side chain of the C-terminal domain residue Tyr404.



**Figure 2:** Co-crystal structure of *P. fluorescens* KMO in complex with **31**. Enzyme residues (grey) surrounding the bound inhibitor (orange) are shown in stick representation, with hydrogen bonds shown as dashed lines (red). Heteroatoms are coloured according to atom type: nitrogen (blue), oxygen (red), sulfur (yellow) and chlorine (green). FAD, flavin adenine dinucleotide.

The 5-chlorine substituent, critical for good activity within this series and several other series of KMO inhibitors (exemplified in Figure 1), forms two types of interactions (Figure 3). Firstly, an interaction (coloured cyan) from a Phe319 aromatic ortho hydrogen ( $\delta +ve$ ) to the “side” of the chlorine atom ( $\delta -ve$ ), and secondly, an interaction (coloured purple) from the  $\pi$  cloud of the Phe 238 aromatic ring ( $\delta -ve$ ) and the sigma hole “end” of the chlorine atom ( $\delta +ve$ ). Both these types of interactions are observed for chlorine atoms interacting with electron-rich and electron-poor centres in crystal structures in the Cambridge Structural Database, and are supported by high level *ab initio* quantum mechanics studies.<sup>21-22</sup> The nature of these interactions reveal why only a bromine atom (which also has a  $\delta +ve$  sigma hole in this position) is able to deliver similar activity, and why methyl substitution is considerably less potent.

**Figure 3:** Interaction of 5-chlorine atom substituent with Phe238 and Phe319

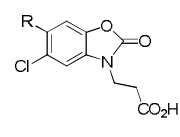
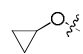




The co-crystal structure indicated that further exploration was likely to be limited to substitution on the 6-position of the benzoxazolone occupying a lipophilic pocket close to the FAD co-factor. Indeed, a range of groups were tolerated although substitution was sensitive to electronic effects and lipophilicity. A polar nitrile substituent was detrimental for enzyme potency and approximately 10-fold weaker than the corresponding methyl compound **30** (Table 5). The lipophilic CF<sub>3</sub> group was also weaker than **30**, and this decrease in activity may reflect the impact of the electron-withdrawing nature of the CF<sub>3</sub> group on the H-bonding interaction between the adjacent chlorine atom and the CH of Phe319. Ethyl substitution maintained good levels of enzyme and cellular inhibition (pIC<sub>50</sub> 6.5), albeit with an increase in HSA binding. The isopropyl compound **35** was significantly weaker confirming the steric restrictions in this pocket.

Substitution at the 6-position with alkoxy groups followed a similar trend in enzyme activity. Methoxy and ethoxy compounds **36** and **37** were tolerated, achieving excellent levels of enzyme inhibition. As observed with compounds **21** and **30**, increasing lipophilicity led to a dramatic increase in cellular potency; the ethoxy analogue **37** was 10-fold more potent than the methoxy compound **36**, suggesting that, within this series of carboxylic acids, the lipophilicity of **37** may approach the value required for optimum cellular penetration.

**Table 5:** Profiles of key benzoxazolones

	R	KMO Enzyme <sup>15</sup> mean pIC <sub>50</sub> (n)	KMO Cell <sup>3</sup> mean pIC <sub>50</sub> (n)	MW / ChromlogD pH 7.4 <sup>17</sup>	HT Sol (μM) <sup>18</sup>	HSA binding <sup>19</sup> (%)
<b>32</b>	CN	7.0 (5)	4.1 (2)	267 / 0.5	>= 441	78.2
<b>33</b>	CF <sub>3</sub>	7.4 (5)	4.8 (4)	310 / 2.1	296	96.9
<b>34</b>	CH <sub>3</sub> CH <sub>2</sub>	8.0 (7)	6.5 (4)	270 / 1.9	295	97.4
<b>35</b>	(CH <sub>3</sub> ) <sub>2</sub> CH	7.0 (6)	5.7 (2)	284 / 2.4	299	98.6
<b>36</b>	CH <sub>3</sub> O	7.9 (8)	5.3 (2)	272 / 0.8	422	89.0
<b>37</b>	CH <sub>3</sub> CH <sub>2</sub> O	8.3 (5)	6.4 (7)	286 / 1.5	>= 332	88.7
<b>38</b>	(CH <sub>3</sub> ) <sub>2</sub> CHO	7.1 (2)	5.8 (5)	300 / 1.9	>= 299	92.2
<b>39</b>		8.5 (5)	5.9 (8)	298 / 1.6	>= 375	94.3

Data are given for the 2-amino-(2-hydroxymethyl)-propane-1,3-diol salt except for **32** and **36** which are given for the parent acids

The cyclopropyl analogue **39** regained approximately 30-fold increase in enzyme potency compared to the isopropyl analogue **38**, mirroring SAR found within the pyrimidine series **5** reported by CHDI /

Evotec.<sup>14</sup> The difference in potency can possibly be rationalised from the *P. fluorescens* KMO co-crystal structure of **39**, which showed that the cyclopropyl group lies immediately adjacent to the FAD isoalloxazine ring C6, whereas the isopropyl hydrogens in **38** would clash with the C6 hydrogen. In line with our cellular data, Evotec also found that the cellular potencies of the isopropyl and cyclopropyl pyrimidine analogues were surprisingly similar given the large difference in the enzyme inhibitory activity. Such discrepancies in the biochemical and cell potencies may reflect subtle differences between the FAD region of the protein in the recombinant KMO construct and that expressed in the HEK cells.

**30** offered the preferred overall profile from this series, displaying good cell inhibition and free fraction in human plasma (2.4%). **30** formed a crystalline salt with 2-amino-(2-hydroxymethyl)-propane-1,3-diol, which possessed excellent solubility commensurate with intravenous administration (>25mg/mL in 0.9%w/v sodium chloride solution). Further *in vitro* profiling showed negligible inhibition of any of the related enzymes in the tryptophan pathway (<20% inhibition at 100µM against indoleamine-2,3-dioxygenase (IDO), tryptophan-2,3-dioxygenase (TDO), kynurenine aminotransferase-1 and -2 (KAT1 and KAT2), and kynureninase (KYNU)) and against a panel of more than 50 unrelated proteins (IC<sub>50</sub> > 30µM). **30** was not mutagenic in the Ames assay or in the mouse lymphoma L5178Y TK+/- screen when tested in the presence and absence of S9-mix. Structural and mechanistic insights on the mode of action of **30** will be presented elsewhere.<sup>23</sup>

**30** demonstrated good metabolic stability across species in microsomes (< 0.01 mL/min/mg) and hepatocytes (<0.01 mL/min/million of cells). Following a single bolus intravenous dose of the 2-amino-(2-hydroxymethyl)-propane-1,3-diol salt (0.9mg/kg) in the rat, **30** showed limited volume of distribution (0.52 L/kg), low clearance (4.7ml/min/kg) and a half-life of 3.7h. **30** had slightly lower cellular potency against the rat enzyme than the human enzyme (pIC<sub>50</sub> 5.9).

**30** is largely excluded from erythrocytes, giving a mean blood:plasma ratio in rat of 0.56, and is weakly bound by rat plasma proteins, with a free fraction of 9.5%. These parameters suggest that a total blood concentration of 6µM should deliver half maximal inhibition of KMO activity *in vivo*.

Bolus injection of four escalating doses (1, 3, 10 and 30mg/kg) of **30** gave increases in the Kyn concentration that increased in magnitude and duration with dose (Figure 4). These profiles suggest that drug levels of 5-9 µM are required in blood *in vivo* to inhibit the KMO activity by 50%, exactly in line with the potency predicted from *in vitro* data described above.

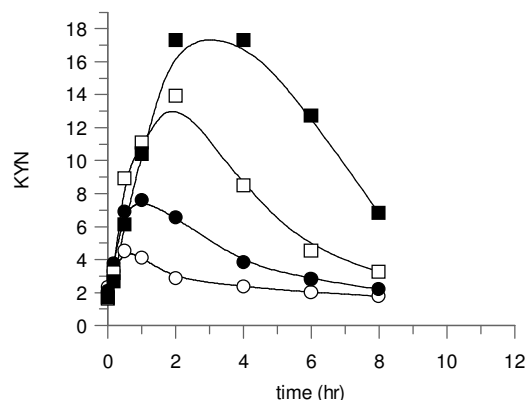
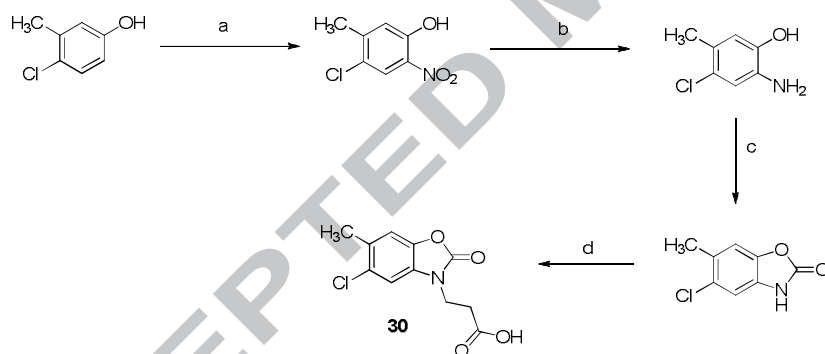


**Figure 4:** Kynurenine concentrations following intravenous administration of **30** (1, 3, 10 and 30mg/kg) to rats

Compounds described herein were prepared using standard procedures, following previously described chemistry, as illustrated below for compound **30**.<sup>24</sup>



**Scheme 1.** Synthesis of **30**. Reagents, conditions and yields. (a) 70% nitric acid, acetic acid, -30 °C then rt, 1 h, 47%; (b) Iron trichloride, active C, methanol,  $\text{NH}_2\text{NH}_2 \cdot \text{H}_2\text{O}$ , 80 °C for 15 h, 79%; (c) 1,1'-carbonyldiimidazole, THF, 66 °C, 1 h, 86%; (d) 3-bromopropanoic acid, potassium carbonate, acetonitrile, 80 °C, 18 h, 65%.

In conclusion, a series of potent, competitive and highly selective KMO inhibitors have been discovered via a substrate-based approach. **30** demonstrated good cellular potency and clear pharmacodynamic activity *in vivo*. Importantly, this class of KMO inhibitors have excellent aqueous solubility amenable for intravenous administration and treatment of AP in a critical care setting. Our subsequent efforts to optimise cell activity and to deliver a clinical candidate will be reported in due course.<sup>25</sup>

## Acknowledgements

The authors thank Paul Homes and Clare Hobbs for preparation of the *Pseudomonas* KMO protein.

This work was funded by GlaxoSmithKline. The human biological samples were sourced ethically and their research use was in accord with the terms of the informed consents. All animal studies were ethically reviewed and carried out in accordance with Animals (Scientific Procedures) Act 1986 and the GSK Policy on the Care, Welfare and Treatment of Animals. All animal studies were ethically reviewed and carried out in accordance with European Directive 86/609/EEC and the GSK Policy on the Care, Welfare and Treatment of Animals.

## References and notes

1. Mole, D. J.; Gungabissoon, U.; Johnston, P.; Cochrane, L.; Hopkins, L.; Wyper, G. M. A.; Skouras, C.; Dibben, C.; Sullivan, F.; Morris, A.; Ward, H. J. T.; Lawton, A. M.; Donnan, P. T. *BMJ Open* **2016**, 6:e011474. doi:10.1136/bmjopen-2016-011474.
2. Christos, S.; Zheng, X.; Binnie, M.; Homer, N. Z. M.; Murray, T. B. J.; Robertson, D.; Briody, L.; Paterson, F.; Spence, H.; Derr, L.; Hayes, A. J.; Tsoumanis, A.; Lyster, D.; Parks, R. W.; Garden, O. J.; Iredale, J. P.; Uings, I. J.; Liddle, J.; Wright, W. L.; Dukes, G.; Webster, S. P.; Mole, D. J. *Scientific Reports* 6, Article number: 33951 (2016) doi:10.1038/srep33951
3. Mole, D. J.; Webster, S. P.; Uings, I.; Zheng, X.; Binnie, M.; Wilson, K.; Hutchinson, J. P.; Mirguet, O.; Walker, A.; Beaufile, B.; Ancellin, N.; Trotter, L.; Bénétou, V.; Mowat, C. G.; Wilkinson, M.; Rowland, P.; Haslam, C.; McBride, A.; Homer, N. Z. M.; Baily, J. E.; Sharp, M. G. F.; Garden, O. J.; Hughes, J.; Howie, S. E. M.; Holmes, D. H.; Liddle, J.; Iredale, J. P. *Nature Medicine* **2016**, 22 (2), 202-209.
4. Crozier-Reabe, K. R.; Phillips, R. S.; Moran, G. R. *Biochemistry* **2008**, 47, 12420-12433
5. Smith, J. R.; Jamie, J. F.; Guillemín, G. J. *Drug Discovery Today* **2015**, 21(2), 315-24
6. Amaral, M.; Levy, C.; Heyes, D. J.; Lafite, P.; Outeiro, T. F.; Giorgini, F.; Leys, D.; Scrutton, N. S. *Nature* **2013**, 496, 382-385.
7. Courtney, S.; Scheel, A.; *Top. Med. Chem.* **2010**, 6, 149-176.
8. Stone, T. W.; Darlington, L. G.; *Nat. Rev. Drug Discov.* **2002**, 1, 609.
9. Pellicciari, R.; Natalini, B.; Costantino, G.; Mahmoud, M. R.; Mattoli, L.; Sadeghpour, B. M.; Moroni, F.; Chiarugi, A.; Carpenedo, R. *J. Med. Chem.*, **1994**, 37 (5), 647-655.
10. Sapko, M. T.; Guidetti, P.; Yu, P.; Tagle, D. A.; Pellicciari, R.; Schwarcz, R. *Exp Neurol.* **2006**, 197, 31-40.
11. Drysdale, M. J.; Hind, S. L.; Jansen, M.; Reinhard, J. F. *J. Med. Chem.*, **2000**, 43, 123-127.
12. Giordani, A.; Pevarello, P.; Cini, M.; Bormetti, R.; Greco, F.; Toma, S.; Speciale, C.; Varasi, M. *Bioorg. Med. Chem. Lett.* **1998**, 8, 2907-2912.
13. Röver, S.; Cesura, A. M.; Huguenin, P.; Kettler, R.; Szente, A. *J. Med. Chem.* **1997**, 40, 4378-4385
14. Toledo-Sherman, L. M.; Prime, M. E.; Mrzljak, L.; Beconi, M. G.; Beresford, A.; Brookfield, F. A.; Brown, C. J.; Cardaun, I.; Courtney, S. M.; Dijkman, U.; Hamelin-Flegg, E.; Johnson, P. D.; Kempf, V.; Lyons, K.; Matthews, K.; Mitchell, W. L.; O'Connell, C.; Pena, P.; Powell, K.; Rassoulpour, A.; Reed, L.; Reindl, W.; Selvaratnam, S.; Friley, W. W.; Weddell, D. A.; Went, N. E.; Wheelan, P.; Winkler, C.; Winkler, D.; Wityak, J.; Yarnold, C. J.; Yates, D.; Munoz-Sanjuan, I.; Dominguez, C. *J. Med. Chem.* **2015**, 58 (3), 1159-1183.
15. Lowe, D. M.; Gee, M.; Haslam, C.; Leavens, B.; Christodoulou, E.; Hissey, P.; Hardwicke, P.; Argyrou, A.;

- Webster, S. P.; Mole, D. J.; Wilson, K.; Binnie, M.; Yard, B. A.; Dean, T.; Liddle, J.; Uings, I.; Hutchinson, J. P. *Journal of Biomolecular Screening*, 2014, 19 (4), 508-515.
16. Abadzapatero, C.; Metz, J. *Drug Discovery Today* **2005**, 10 (7): 464–469
  17. Young, R. J.; Green, D. V. S.; Luscombe, C. N.; Hill, A. P. *Drug Discovery Today*, **2011**, 16, 822-830.
  18. 5ml of 10mM DMSO stock solution diluted to 100ul with pH7.4 phosphate buffered saline, equilibrated for 1 hour at room temperature, filtered through Millipore Multiscreen<sub>HTS</sub>-PCF filter plates (MSSL BPC). The filtrate is quantified by suitably calibrated flow injection Chemi-Luminescent Nitrogen Detection
  19. Valko, K.; Nunhuck, S.; Bevan, C.; Abraham, M. H.; Reynolds, D. P.; *J. Pharm. Sci.* **2003**, 92, 2236–2248
  20. The protein production, crystallisation, crystal soaking and structure determination were carried out using the methods described in Hutchinson *et al.* (manuscript in preparation). The X-ray data were collected at the European Synchrotron Radiation Facility (ESRF). The coordinates and structure factors have been deposited in the Protein Data Bank under the accession code 5N7T.
  21. Wilcken, R.; Zimmermann, M. O.; Lange, A.; Joerger, A. C; Boeckler, F. M. *J. Med. Chem.* **2013**, 56, 1363-1388.
  22. Bissantz, C.; Kuhn, B.; Stahl, M. *J Med. Chem.* **2010**, 53, 5061–5084
  23. Hutchinson *et al.* (manuscript in preparation).
  24. Bouillot, A. M. J.; Mirguet, O.; Liddle, J.; Walker, A. L. **2015**, WO 2015091647.
  25. Walker *et al.* (manuscript in preparation).

Kynurenine  
Substrate

GSK428

KMO  $\text{pIC}_{50}$  : 7.9

